Photoinduced Intramolecular n−π* Electron Transfer in Aminofullerene Derivatives

Ya-Ping Sun,* Bin Ma, and Christopher E. Bunker[†]

Department of Chemistry, Howard L. Hunter Chemistry Laboratory, Clemson University, Clemson, South Carolina 29634-1905

Received: June 11, 1998; In Final Form: July 20, 1998

The photophysical properties of two amino-C_{60} derivatives, which are adducts of C_{60} with *N,N′*-dimethyl-1,2-ethylenediamine and C_{60} with piperazine, were studied systematically. The results show that there is intramolecular n (amino groups) to π* (photoexcited fullerene cage) electron transfer in the aminofullerene molecules. The photoinduced electron transfer can be observed only in a polar solvent environment for the first compound and also in polarizable solvents for the second compound. As a result, the fluorescence quantum yields and lifetimes and the nonlinear absorptive optical limiting responses of the amino-C_{60} derivatives are strongly solvent dependent. Charge-transfer excited states are formed following electron transfer in both compounds, but only that of the second compound is emissive. There is also evidence for delayed fluorescence in polar solvents, which is probably due to the vertical excited singlet state repopulated from the charge-transfer excited state. However, the fluorescence quenchings and effects on optical limiting in polar solvents can be eliminated through protonating amino groups in the molecules by adding a small amount of trifluoroacetic acid into the sample solutions. Although the intramolecular n−π* electron transfer in aminofullerenes shares some characteristics with the classical twisted intramolecular charge transfer in molecules represented by *p-N,N*-dimethylaminobenzonitrile, the amino-C_{60} derivatives are in fact better classified as redox dyads. Since electron donor (amino groups) and acceptor (fullerene cage) are linked directly through only sp^3 carbons, these are the simplest donor−spacer−fullerene dyads. In more quantitative treatments, electron-transfer rate constants for the amino-C_{60} derivatives under different solvent conditions were correlated with the solvent microscopic polarities, which were estimated using the strongly solvatochromic molecular probe 6-propionyl-2-(*N,N*-dimethylamino)naphthalene.

Introduction

Photoinduced electron transfer and charge separation have been studied extensively.[1,2] Among classical examples for intramolecular n−π* electron transfer are molecules represented by *N,N*-dimethylaminobenzonitrile (DMABN) that undergo twisted intramolecular charge transfer (TICT) upon photoexcitation.[3−5] In the TICT molecules, twisting in the excited state that results in essentially an orthogonal relationship between the n and π* orbitals and a polar solvent environment are necessary for the electron transfer and the formation of a charge-transfer excited state. In addition, electron-withdrawing substitution on the π moiety is typically required.[4,5]

Fullerenes are excellent electron acceptors, especially in the photoexcited states.[6−8] Fluorescence emissions of fullerene molecules are quenched efficiently by electron donors such as aromatic amines.[9−14] Stern−Volmer plots for quenchings of fullerene fluorescence intensities by aromatic amines often exhibit significant upward deviations even at moderate quencher concentrations, and the deviations are attributed to contributions of static quenching.[10,12] A somewhat special feature in the photoinduced fullerene−amine electron transfer is the extremely strong solvent dependence. In aliphatic hydrocarbon solvents such as hexane and methylcyclohexane, quenchings of C_{60} and C_{70} fluorescence intensities by aromatic amines are accompanied by the formation of emissive exciplexes.[9,12] However, exciplex emissions are absent for the same fullerene−amine systems in toluene and CS_2 or in a solvent mixture containing a small fraction of a polar component such as THF or methylene chloride.[13] It was concluded that the extreme solvent dependence is related to the polarity and polarizability of the solvent rather than to specific fullerene−solvent interactions.[13] The conclusion is consistent with recent results concerning emissive exciplexes of methano- or pyrrolidino-C_{60} derivatives and aromatic amines.[15,16] For the C_{60} derivatives, emissions from the fullerene−amine exciplexes can be observed in both aliphatic and aromatic hydrocarbon solvents. However, the exciplex emissions are completely quenched in a somewhat more polar solvent environment such as a hexane/acetone or toluene/acetonitrile solvent mixture.[15,16]

Recently, studies of photoinduced intramolecular electron transfer in fullerene-based dyads and triads with different donors and bridges (or spacers) have been reported.[17−23] Issues under consideration include mechanistic details on quenchings of fullerene excited states through intramolecular electron transfer and effects of the bridge length and geometry on the electron-transfer process. In addition, photoinduced intrapolymer electron transfer and its solvent dependence in fullerene-containing polymeric materials have also been studied.[24,25] Here we report a systematic molecular spectroscopic investigation of two amino-C_{60} derivatives concerning the photoinduced nontwisting intramolecular n−π* electron transfer in the molecules and the high sensitivity of the electron-transfer process to changes in solvent environment. The results are compared with those of a pyrrolidino-C_{60} derivative in which the electron-transfer process is absent. The difference in donor−acceptor interactions

[†] Current address: Aero Propulsion and Power Directorate, Wright Laboratory, Wright-Patterson Air Force Base, OH 45433.

S1089-5639(98)02591-2 CCC: $15.00
Published on Web 09/09/1998

between the amino- and pyrrolidino-C_{60} derivatives, which all contain amino groups, is discussed in terms of their molecular structures calculated using both semiempirical and ab initio methods. Since there are no ground-state interactions between amino groups and the fullerene cage in the molecules, the amino-C_{60} derivatives are in fact better classified as electron donor−acceptor dyads with one of the simplest bridges. Thus, the aminofullerene molecules may serve as models for more complex fullerene-based redox systems.

Experimental Section

Materials. C_{60} (purity > 99.5%) was obtained from Bucky-USA and was used without further purification. All solvents are of spectrophotometry grade. Because there is no interference of possible impurities in the wavelength range of interest according to absorption and emission spectroscopic measurements, the solvents were used as received.

Amino-C_{60} Derivatives I and II. The compound **I** was prepared in the photochemical reaction of C_{60} and *N*,*N*′-dimethyl-1,2-ethylenediamine. The photoirradiation was carried out using an ACE Glass Co. ACE-7861 type immersion well photochemical reaction assembly equipped with a 450-W Hanovia medium-pressure mercury lamp. A solution of 518 mg (5.9 mmol) *N*,*N*′-dimethyl-1,2-ethylenediamine in 40 mL of toluene was added dropwise with stirring to a solution of 580 mg (0.81 mmol) of C_{60} in 260 mL toluene in the reaction vessel. The solution mixture was purged with dry nitrogen gas for ∼1 h before photoirradiation, and the loss of solvent during the nitrogen purging was prevented by attaching a condenser to the outlet of the reaction vessel. An aqueous solution of potassium chromate (0.1 g/mL) was used as a liquid cutoff filter (505 nm). The photoirradiation was continued for 70 min under a nitrogen atmosphere. The solution was then put on a rotavap to remove the solvent toluene. The solid reaction mixture was extracted repeatedly using CS_2. The CS_2 solution was then concentrated and separated on a silica gel column using hexane/50% v/v toluene, methylene chloride, and then methylene chloride−0.8% v/v methanol as eluents, yielding 150 mg of the amino-C_{60} derivative **I** (23% yield). The compound was positively identified by matrix-assisted laser desorption ionization time-of-flight (MALDI-TOF) MS and proton and ^{13}C NMR characterizations.[26]

The amino-C_{60} derivative **II** was prepared in a similar photochemical reaction of C_{60} with piperazine in toluene solution. The separation and purification procedures are the same as those used for **I**. The compound **II** was also positively identified by MALDI-TOF MS and NMR characterizations.[26,27]

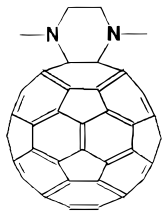

I

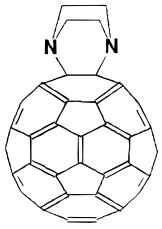

II

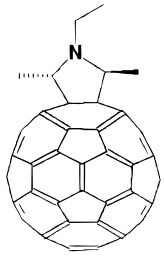

III

The samples used in spectroscopic measurements were purified through repeated washing with toluene on a short silica gel column. The sample purity was checked in HPLC analyses using a BuckyCluch column (Regis Technologies, Inc.), and only one peak was found for each of the samples.

Pyrrolidino-C_{60} Derivative III. The compound **III** was obtained from a photochemical reaction of C_{60} with triethylamine in toluene solution. The purification and structural characterization of the compound have been reported elsewhere.[28]

Measurements. Absorption spectra were obtained using a computer-controlled Shimadzu UV2101-PC spectrophotometer. Emission spectra were recorded on a Spex Fluorolog-2 photon-counting emission spectrometer equipped with a 450-W xenon source, a Spex 340S dual-grating and dual-exit emission monochromator, and two detectors. The two gratings are blazed at 500 nm (1200 grooves/mm) and 1000 nm (600 grooves/mm). The room-temperature detector consists of a Hamamatsu R928P photomultiplier tube operated at −950 V, and the thermoelectrically cooled detector consists of a near-infrared-sensitive Hamamatsu R5108 photomultiplier tube operated at −1500 V. In fluorescence measurements, a Schott 540 nm (GG-540) or 610 nm (RG-610) color glass sharp-cut filter was placed before the emission monochromator to eliminate the excitation scattering. Minor distortion at the blue onset of the observed fluorescence spectra due to the filter was corrected by use of the transmittance profile of the filter. The slit of the excitation monochromator was 5 mm (19 nm resolution). For the emission monochromator, a wide slit of 5 mm (19 nm resolution) was used in fluorescence quantum yield measurements to reduce experimental uncertainties, and a narrow slit of 0.5 mm (2 nm resolution) was used in fluorescence spectral measurements to retain structures of the spectra. Unless specified otherwise, fluorescence spectra were corrected for nonlinear instrumental response by use of predetermined correction factors. The correction factors for the emission spectrometer were carefully determined using a calibrated radiation standard from Optronic Laboratories.

Fluorescence decays were measured using time-correlated single photon counting (TCSPC) method. The TCSPC setup consists of a Hamamatsu stabilized picosecond light pulser (PLP-02) as the excitation source, which produces ∼33 ps (fwhm) light pulses at 632 nm with a repetition rate of 1 MHz. Fluorescence decays were monitored through a 695 nm color glass sharp-cut filter. The detector consists of a Hamamatsu R928P photomultiplier tube operated at −1 kV using an EG&G Ortec 556 high-voltage power supply. The detector electronics from EG&G Ortec include two 9307 discriminators, a 457 biased time-to-amplitude converter, and a 916A multichannel analyzer. The instrument response function of the setup has a fwhm of ∼1.2 ns. Fluorescence lifetimes were determined from observed decay curves and instrument response functions through deconvolution by use of the Marquardt nonlinear least-squares method.

The setup for optical limiting measurements[29,30] consists of a Continuum Surelite-I Q-switched Nd:YAG laser operated in the single-shot mode. The infrared fundamental was frequency-doubled to generate the second harmonic at 532 nm. It was isolated by use of a Surelite harmonic separation package. The maximum energy at 532 nm is 160 mJ/pulse with a 5 ns pulse width (fwhm). The laser output was varied in a range of 10−160 mJ/pulse using a waveplate/polarizer combination. The laser beam has a diameter of 6 mm, corresponding to energy densities of 0.035−0.57 J/cm^2. A Galilean style telescope consisting of a planoconcave lens and a planoconvex lens was used to reduce the laser beam waist to 3 mm in diameter for higher energy densities up to 2.2 J/cm^2. A Scientech Mentor MC2501 calorimeter and a MD10 meter were used as the

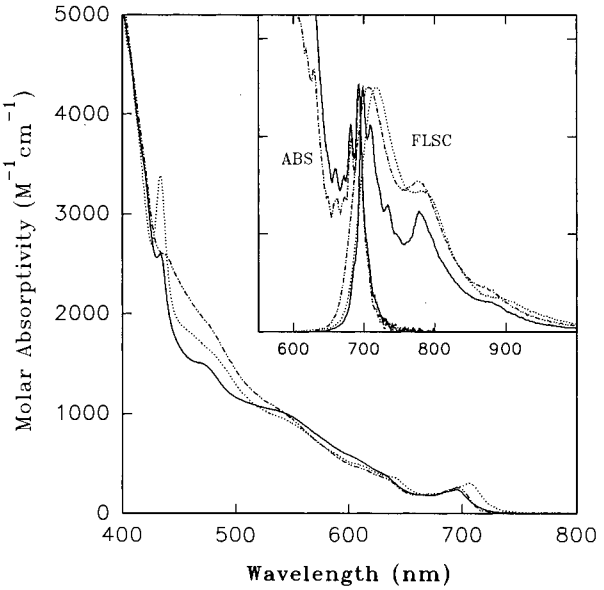

Figure 1. Absorption spectra of the amino-C_{60} derivatives **I** (- ·· -) and **II** (—) and the pyrrolidino-C_{60} derivative **III** (···) in room-temperature toluene. Shown in the inset are absorption and fluorescence spectra of the molecules in room-temperature hexane.

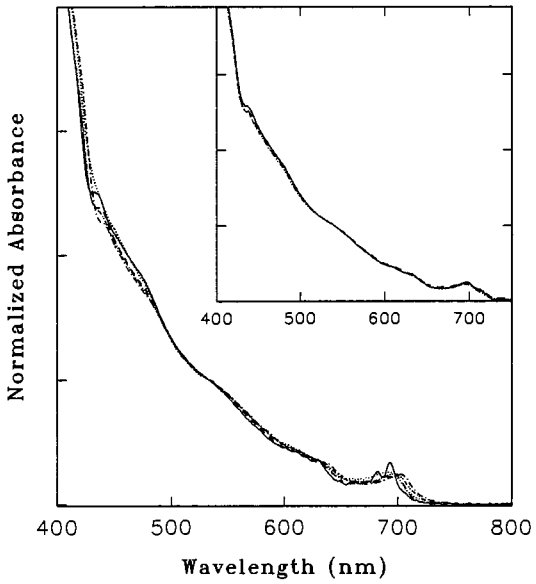

Figure 2. Absorption spectra of **I** in hexane (—), toluene (- - -), chloroform (···), *o*-dichlorobenzene (- ·· -), and CS_2 (- · -). Shown in the inset are absorption spectra of **I** in toluene/acetonitrile mixtures with acetonitrile volume fractions of 0 (—), 10 (- - -), 20 (···), and 30% (- · -).

detector. Solution samples were measured in a cuvette with a 2 mm optical path length.

Computations for optimized geometries of the amino-C_{60} derivatives were carried out on a Silicon Graphics workstation. The semiempirical and ab initio calculations were performed in the environment of commercial software packages Spartan (version 3.0) from Wavefunction Inc. and Gaussian-94 from Gaussian Inc.

Results

UV/vis Absorption. UV/vis absorption spectra of the amino-C_{60} derivatives **I** and **II** in toluene at room temperature (22 °C) are shown in Figure 1. The two spectra show similar features, with the weak 0−0 absorption band at ∼695 nm in both spectra. Also shown in Figure 1 for comparison is the absorption spectrum of pyrrolidino-C_{60} derivative **III** in toluene. While the amino- and pyrrolidino-C_{60} derivatives share some common absorption features, an obvious difference is that the sharp absorption peak at ∼430 nm in the spectrum of the pyrrolidino-C_{60} derivative is absent in the spectra of amino-C_{60} derivatives (Figure 1).

Absorption spectra were also measured for the amino-C_{60} derivatives **I** and **II** in a series of solvents of different polarities and polarizabilities and in solvent mixtures. Shown in Figure 2 are absorption spectra of **I** in several representative solvents and in toluene/acetonitrile mixtures. The absorption spectra are apparently insensitive to solvent changes, except for minor solvatochromic shifts and a better spectral resolution in hexane. The results for **II** in different solvents are similar (Figure 3).

Fluorescence Spectra. Fluorescence spectra of the amino-C_{60} derivatives were measured in room-temperature hexane. The spectrum of **II** shows fine structures, with peaks at 699, 709, 734, and 780 nm and a shoulder at ∼880 nm, but the spectrum of **I** is considerably broader (Figure 1, inset). However, fluorescence spectra of both compounds are in the same emission wavelength region, and the spectra are in excellent mirror image relationships with their corresponding absorption spectra (Figure 1, inset). Also shown in the inset of Figure 1 for comparison is the fluorescence spectrum of pyrrolidino-C_{60} derivative **III** in room-temperature hexane. The spectrum is similar to that of the amino-C_{60} derivative **I**. As expected, fluorescence spectra of all three compounds are excitation wavelength independent.

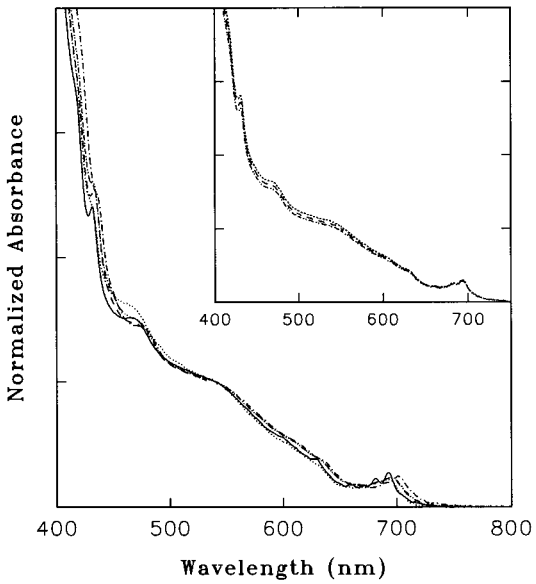

Figure 3. Absorption spectra of **II** in methylcyclohexane (—), toluene (- - -), chloroform (···), *o*-dichlorobenzene (- ·· -), and CS_2 (- · -). Shown in the inset are absorption spectra of **II** in methylcyclohexane/acetone mixtures with acetone volume fractions of 0 (—), 2 (- - -), 6 (···), and 8% (- · -).

Solvent effects on the fluorescence spectral profile were examined systematically by measuring fluorescence spectra of **I** and **II** in solvents of different polarities and polarizabilities and in solvent mixtures. For compound **I**, observed fluorescence spectra are insensitive to changes in solvent environment, except for some solvatochromic shifts (Figures 4 and 5). However, fluorescence spectra of the compound **II** are more strongly solvent dependent. As shown in Figure 6, the fluorescence spectrum of **II** in the methylcyclohexane/acetone (10%, v/v) mixture is not only broader but also more intense at the longer

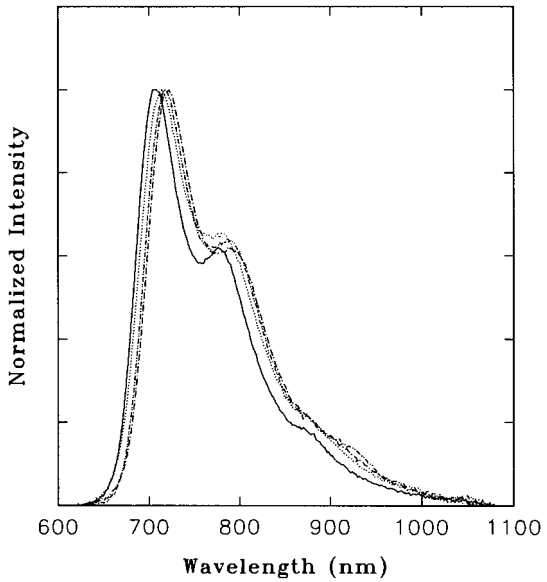

Figure 4. Fluorescence spectra of **I** in hexane (—), chloroform (···), *o*-dichlorobenzene (- ·· -), and CS_2 (- · -).

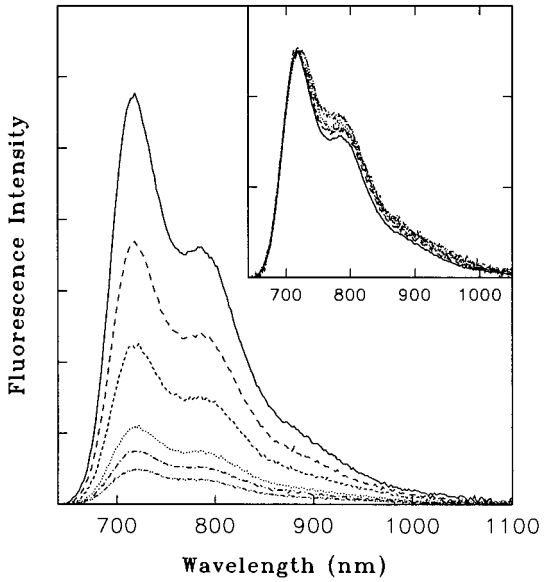

Figure 5. Fluorescence spectra (normalized in the inset) of **I** in toluene/acetonitrile mixtures with acetonitrile volume fractions of 0 (—), 5 (— — —), 10 (- - -), 20 (···), 30 (- · -), and 40% (- ·· -).

wavelength side in comparison with the spectrum of **II** in neat methylcyclohexane. For the pyrrolidino-C_{60} derivative **III**, the solvent dependence of the fluorescence spectral profile is similar to that for **I**, with the observed spectra exhibiting only minor solvatochromic shifts from solvent to solvent.

Fluorescence Quantum Yields. Fluorescence quantum yields of the amino-C_{60} derivatives **I** and **II** in room-temperature hexane were determined in reference to that of C_{60} ($\Phi_F = 3.3 \times 10^{-4}$).[31] Both **I** and **II** are more fluorescent than C_{60}, with their fluorescence quantum yields larger than that of C_{60} by approximately a factor of 3, which is typical for many C_{60} derivatives including **III**.[15,30,32] However, while the fluorescence quantum yield of the pyrrolidino-C_{60} derivative **III** is little affected by changes in solvent conditions,[15] fluorescence quantum yields of both amino-C_{60} derivatives **I** and **II** are strongly solvent dependent. As summarized in Table 1 for **I** under different solvent conditions, fluorescence yields are generally smaller in more polar solvents. For example, the yield

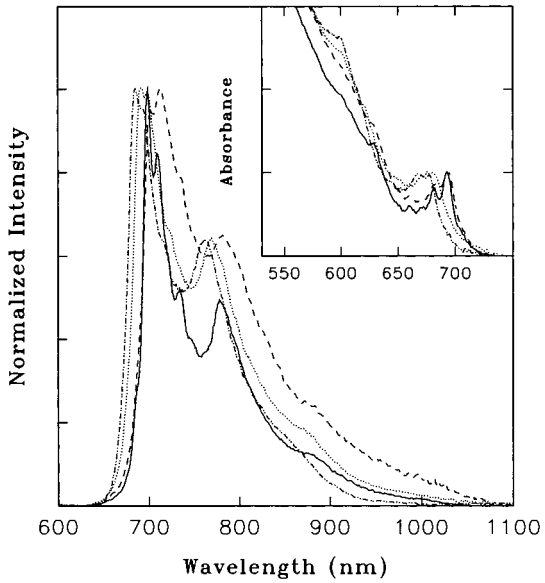

Figure 6. Absorption (the inset) and fluorescence spectra of **II** in methylcyclohexane (MCH, —) and mixtures of MCH/10% acetone (- - -), MCH/10% acetone−2% TFA (···), and MCH−2% TFA (- ·· -).

TABLE 1: Fluorescence Quantum Yields and Lifetimes of I under Different Solvent Conditions

solvent	dielectric constant[a]	Φ_F ($\times 10^4$)	τ_{F1} (ns)	τ_{F2} (ns)
hexane	1.89	11	1.4	
toluene	2.38	9.1	1.3	
o-xylene	2.57	10	1.3	
1,2,4-trimethylbenzene	2.26	10	1.4	
1,2,3,5-tetramethylbenzene	2.29	10	1.4	
carbon disulfide	2.64	7.0	1.1[b]	
chloroform	4.81	8.5	1.2[b]	
THF	7.58	2.0	0.17	1.5
dichloromethane	8.93	5.3	0.54	1.4
dichloromethane + 1% TFA		8.3	1.3	
dichlorobenzene	9.93	6.6	1.0[b]	
toluene + 5%(v/v) acetonitrile	4.00	6.2	0.59[b]	
toluene + 10%(v/v) acetonitrile	5.74	4.0	0.32	1.4
toluene + 20%(v/v) acetonitrile	9.09	2.2	0.16	1.2
toluene + 30%(v/v) acetonitrile	12.5	1.7		
toluene + 40%(v/v) acetonitrile	15.8	1.3		
toluene + 40% acetonitrile + 1% TFA		9.0	1.5	

[a] Dielectric constants of the binary solvent mixtures were estimated by algebraic averaging based on mole fractions. [b] Decay was deconvoluted using a monoexponential equation because the contribution of longer-lived emission is negligible.

in dichloromethane (5.3×10^{-4}) is only about half of those in hexane and toluene. The solvent polarity dependence of the fluorescence quantum yield is more clearly demonstrated by the results of **I** in a series of toluene/acetonitrile mixtures. As the acetonitrile volume fraction in the mixtures increases from 0 to 40%, the fluorescence quantum yield of **I** decreases monotonically from 9.1×10^{-4} to 1.3×10^{-4} (Table 1).

Fluorescence quantum yields of compound **II** are apparently even more solvent sensitive. While the results in hexane and methylcyclohexane are the same, the fluorescence yields become much smaller even in toluene and other solvents of methyl-substituted benzenes (Table 2). In polar solvents, fluorescence quantum yields of **II** are all significantly lower than those in hexane and methylcyclohexane. The solvent polarity dependence of the fluorescence quantum yield is also more evident for **II** in polar solvent mixtures. When a small amount of polar

TABLE 2: Fluorescence Quantum Yields and Lifetimes of II under Different Solvent Conditions

solvent	dielectric constant[a]	Φ_F ($\times 10^4$)	τ_{F1} (ns)	τ_{F2} (ns)
hexane	1.89	10	1.3	
methylcyclohexane (MCH)	2.02	10	1.3	
toluene	2.38	1.9	0.32	1.7
o-xylene	2.57	2.5	0.41	1.7
1,2,4-trimethylbenzene	2.26	3.5	0.41	1.4
1,2,3,5-tetramethylbenzene	2.29	4.5	0.52	1.6
carbon disulfide	2.64	5.7	1.0	1.4
chloroform	4.81	3.9	0.44	1.6
THF	7.58	<0.5	<0.1	
dichloromethane	8.93	<0.5	<0.1	
dichlorobenzene	9.93	~1.0	0.2	1.7
hexane + 10%(v/v) THF	2.76	3.7		
hexane + 10%(v/v) acetone	4.98	1.7		
hexane + 10%(v/v) ethanol	6.40	4.2		
MCH + 10%(v/v) acetone	5.02	1.3	0.32	1.7
MCH + 10%(v/v) acetone + 1%(v/v) TFA		8.3	1.4	

[a] Dielectric constants of the binary solvent mixtures were estimated by algebraic averaging based on mole fractions.

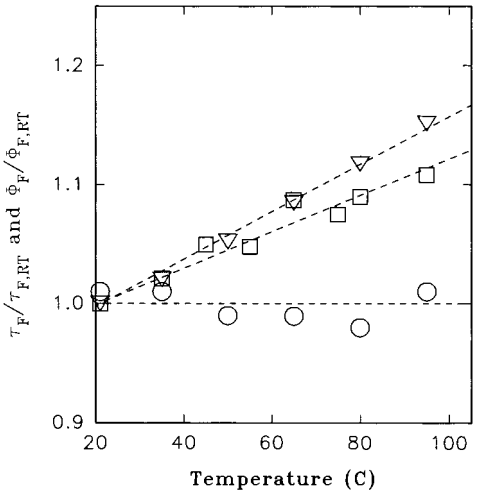

Figure 7. Fluorescence lifetimes of **I** in the toluene/5% acetonitrile mixture (○) and fluorescence quantum yields of **I** in toluene/acetonitrile mixtures with 5% (▽) and 20% (□) acetonitrile at different temperatures.

solvent is added to the hexane or methylcyclohexane solution of **II**, the fluorescence quantum yield decreases substantially. For example, the fluorescence yield of **II** in the methylcyclohexane/acetone (10%, v/v) mixture is only 13% of that in neat methylcyclohexane (Table 2).

Fluorescence quantum yields of **I** in toluene and in the toluene/acetonitrile mixtures with 5% (v/v) and 20% (v/v) acetonitrile were also determined as a function of temperature. While fluorescence yields of **I** in toluene do not change with temperature, the yields in the toluene/acetonitrile mixtures show steady increases with increasing temperature (Figure 7).

Fluorescence Lifetimes. Fluorescence decays of the amino-C_{60} derivatives **I** and **II** in room-temperature hexane and methylcyclohexane were measured. The decay curves can be deconvoluted from their corresponding instrumental response functions using a monoexponential equation (Figures 8 and 9). The fluorescence lifetimes thus obtained are 1.4 ns for **I** and 1.3 ns for **II**, which are similar to those of other C_{60} derivatives with the fullerene cage monofunctionalized.[15,30,32,33] To examine solvent effects on fluorescence lifetimes in a systematic fashion, fluorescence decays of **I** and **II** were also measured in a series of solvents of different polarities and polarizabilities and in polar

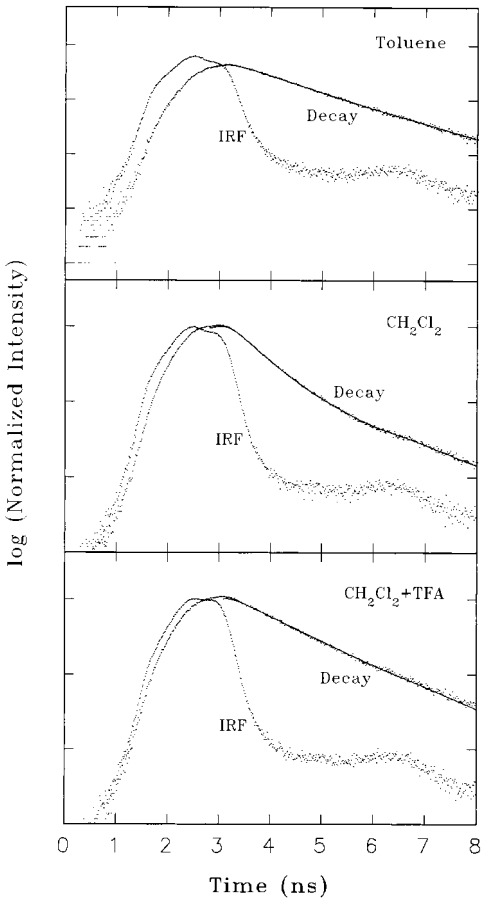

Figure 8. Fluorescence decays of **I** under different solvent conditions. The solid lines are the best-fit results.

solvent mixtures at room temperature. Like fluorescence quantum yields, fluorescence decays of **I** and **II** are both strongly solvent dependent. For compound **I**, the fluorescence lifetime in toluene (1.3 ns) is only slightly shorter than that in hexane. However, the lifetime becomes progressively shorter as the toluene solution is titrated with a polar solvent (Table 1). Similarly short fluorescence lifetimes were obtained for **I** in polar solvents such as THF and dichloromethane. In addition, under polar solvent conditions, the fluorescence decays become difficult to be treated using a monoexponential equation and the presence of a longer-lived component in observed fluorescence decays becomes evident. In dichloromethane, for example, the decay curve can be deconvoluted well from the corresponding instrumental response function using a biexponential equation, with lifetimes of 0.54 and 1.4 ns for the short- and long-lived components, respectively (Figure 8). Under even more polar solvent conditions, such as toluene/acetonitrile mixtures with acetonitrile volume fractions of 30% and 40%, the fluorescence becomes very weak and the decays are too fast for our spectrometer.

Fluorescence lifetimes of **II** under different solvent conditions are summarized in Table 2. While there are clearly similarities in the solvent dependence of fluorescence decays between **I** and **II**, the solvent effects are apparently more extreme for compound **II**. In particular, the fluorescence decay of **II** in toluene is already biexponential, with a lifetime of only 0.32 ns for the short component, which accounts for the bulk of the observed fluorescence intensities. Fluorescence decays of **II** in other polarizable and polar solvents are also biexponential. Lifetimes of the short fluorescence component are different under different solvent conditions, and lifetimes of the long

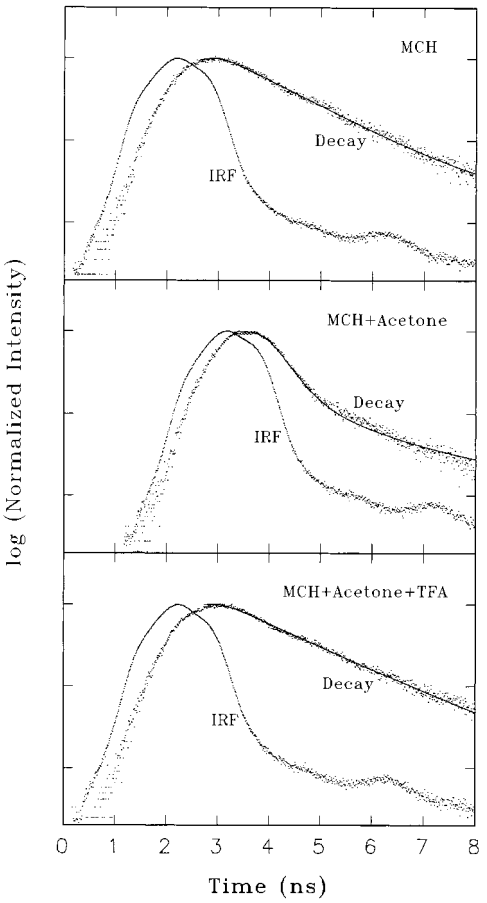

Figure 9. Fluorescence decays of **II** under different solvent conditions. The solid lines are the best-fit results.

fluorescence component vary in a relatively narrow range of 1.4−1.7 ns (Table 2).

Fluorescence decays of compound **I** in the toluene/acetonitrile (5%, v/v) mixture were also measured at different temperatures. As shown in Figure 7, fluorescence lifetimes obtained from the decays are essentially temperature independent.

Optical Limiting. Optical limiting responses of compound **I** in chloroform solution (linear transmittance $T = 55\%$) toward a pulsed (5 ns, fwhm) Nd:YAG laser at 532 nm were measured as a function of the input light fluence. As shown in Figure 10, observed output light fluences from the solution are strongly nonlinear with respect to input light fluences, reaching the onset of a plateau at the input light fluence of ~0.25 J/cm^2. The saturated output light fluences at the plateau are on average ~0.055 J/cm^2, similar to those of other C_{60} derivatives.[29,30] The optical limiting responses are weaker for **I** in a more polar solvent environment in the chloroform/acetonitrile (20%, v/v) mixture (Figure 10). The saturated output light fluences at the plateau (~0.075 J/cm^2 on average) are higher than those for **I** in neat chloroform (Figure 10). Similarly, the optical limiting responses of compound **I** in the toluene/acetonitrile (20%, v/v) mixture are weaker than those of **I** in neat toluene at the same linear transmittance.

Acidification Effects. Photophysical properties of the amino-C_{60} derivatives **I** and **II** are affected strongly by the presence of acid in sample solutions. For compound **I** in dichloromethane, the addition of 1% (v/v) trifluoroacetic acid (TFA) results in blue shifts of both absorption and fluorescence spectra, though the spectral profiles are little affected. Similar acidification effects on absorption and fluorescence spectral profiles were observed for **I** in the toluene/acetonitrile (40%, v/v) mixture.

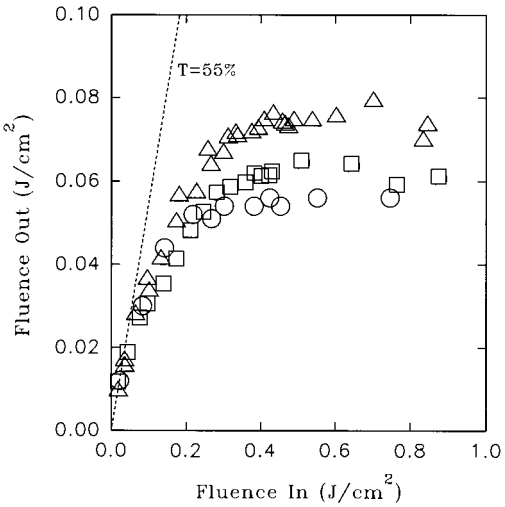

Figure 10. Optical limiting results of **I** in chloroform (○), chloroform/20% acetonitrile (△), and chloroform/20% acetonitrile/1% TFA (□) at room temperature.

Adding TFA to the solutions of **I** in dichloromethane and the toluene/acetonitrile mixture also significantly changes the fluorescence yields and lifetimes of the compound. In the dichloromethane−TFA and toluene−acetonitrile-TFA mixtures with TFA volume fraction of 1%, the fluorescence quantum yields of **I** become 8.3×10^{-4} and 9×10^{-4}, respectively. The fluorescence yields are close to that in neat toluene and much higher than those in the absence of TFA (Table 1). While the fluorescence decay of **I** in dichloromethane solution is biexponential, the decay becomes monoexponential upon the addition of 1% (v/v) TFA. The fluorescence lifetime of **I** in the dichloromethane−TFA mixture is 1.3 ns, the same as that in toluene (Table 1).

Similarly, the absorption spectrum of **II** is also blue-shifted due to TFA in the sample solution (Figure 6). However, the acidification effects on the fluorescence spectra of **II** in polar solvents are noticeably different from those for compound **I**. As shown in Figure 6, the fluorescence spectrum of **II** in the methylcyclohexane/acetone (10%, v/v) mixture undergoes significant changes upon the addition of 2% (v/v) TFA into the sample solution. The spectrum in the presence of TFA becomes narrower, with relatively lower intensities at longer wavelengths. It looks more like the spectrum in neat methylcyclohexane (Figure 6). The fluorescence spectral changes due to TFA are accompanied by a substantial increase in the fluorescence quantum yield. The fluorescence yield of **II** in the methylcyclohexane/acetone mixture with TFA is more than 6 times higher than that in the same solvent mixture without TFA, and it is close to the result of **II** in methylcyclohexane (Table 2). The fluorescence decay of **II** in the presence of TFA again becomes monoexponential, and the fluorescence lifetime of 1.4 ns obtained from the decay is also close to that of **II** in neat methylcyclohexane.

The acidification also affects optical limiting responses of **I** in the polar solvent mixture of chloroform/acetonitrile (20%, v/v). The presence of 1% (v/v) TFA in the solvent mixture noticeably reduces the saturated output light fluences at the plateau, though the limiting performance is still not as good as that in neat chloroform (Figure 10). For compound **I** in the toluene/acetonitrile (20%, v/v) mixture, the presence of 1% (v/v) TFA also significantly improves the optical limiting performance.

Molecular Structures. The ground-state molecular structures of the amino-C_{60} derivatives **I** and **II** were calculated using

TABLE 3: Structural Parameters of Amino Groups in I and II

	MNDO		ab initio	
	I	**II**	**I**	**II**
		Bond Length (Å)		
C1−N1	1.4715	1.5109	1.5006	1.4916
C2−N2	1.4715	1.5109	1.5060	1.4916
C3−N1	1.4704	1.4940	1.4818	1.4940
C4−N2	1.4707	1.4940	1.4870	1.4940
C5−N1	1.4718	1.4940	1.4868	1.4940
C6−N2	1.4695	1.4940	1.4853	1.4940
C1−C2	1.6401	1.6138	1.6220	1.6347
C3−C4	1.5485	1.5619	1.5579	1.5575
C5−C6		1.5619		1.5575
		Bond Angle (deg)		
C1−N1−C3	114.28	109.27	110.07	111.28
C2−N2−C4	115.95	109.27	111.56	111.28
C1−N1−C5	119.22	109.27	114.58	111.27
C2−N2−C6	120.31	109.27	113.72	111.28
C3−N1−C5	115.91	107.70	112.67	108.19
C4−N2−C6	114.45	107.70	114.45	108.19
N1−C1−C2	112.84	109.33	112.93	107.67
N2−C2−C1	107.64	109.33	107.05	107.67
N1−C3−C4	113.70	110.62	113.18	109.20
N2−C4−C3	110.67	110.62	110.02	109.20
N1−C5−C6		110.62		109.20
N2−C6−C5		110.62		109.20

both semiempirical (MNDO)[34] and ab initio (STO-3G minimum base set)[35] methods. Results from the two computational methods are similar. Summarized in Table 3 are the structural parameters calculated using both MNDO and ab initio methods for the amino pieces attaching to the fullerene cage. The ab initio optimized molecular geometries of **I** and **II** are shown in Figure 11. Also shown in the figure for comparison is the ab initio optimized geometry of the pyrrolidino-C_{60} derivative **III**. There are significant differences among the three molecules concerning the relationship between the amino group and the fullerene cage. The ab initio optimized geometry of **III** shows a distance of 5.92 D between the amino nitrogen and the center of the fullerene cage. In the two amino-C_{60} derivatives, each of which has two amino groups, the two nitrogen atoms are symmetric with respect to the center of fullerene cage. The nitrogen−cage center distances in **I** and **II** are 5.05 and 5.06 D, respectively. In addition to the distances, the orientation of nitrogen n orbital (lone pair electrons) with respect to the fullerene cage is also different for different amino groups in the three derivatives. As shown in Figure 11, the nitrogen n orbital in **III** actually points away from the fullerene cage surface. However, the n orbitals on the two amino groups in **I** point to different directions, one away from the cage surface and the other parallel (and closer) to the cage surface. In the optimized geometry of **II**, the two n orbitals are symmetric, both parallel to the fullerene cage surface. The computational molecular structure of **II** is in reasonable agreement with the X-ray crystallographic result reported in the literature.[27]

Discussion

In the ground state, the amino-C_{60} derivatives **I** and **II** behave as other C_{60} derivatives,[15,30,32,33] with electronic transitions dictated by the monofunctionalized fullerene cage. In fact,

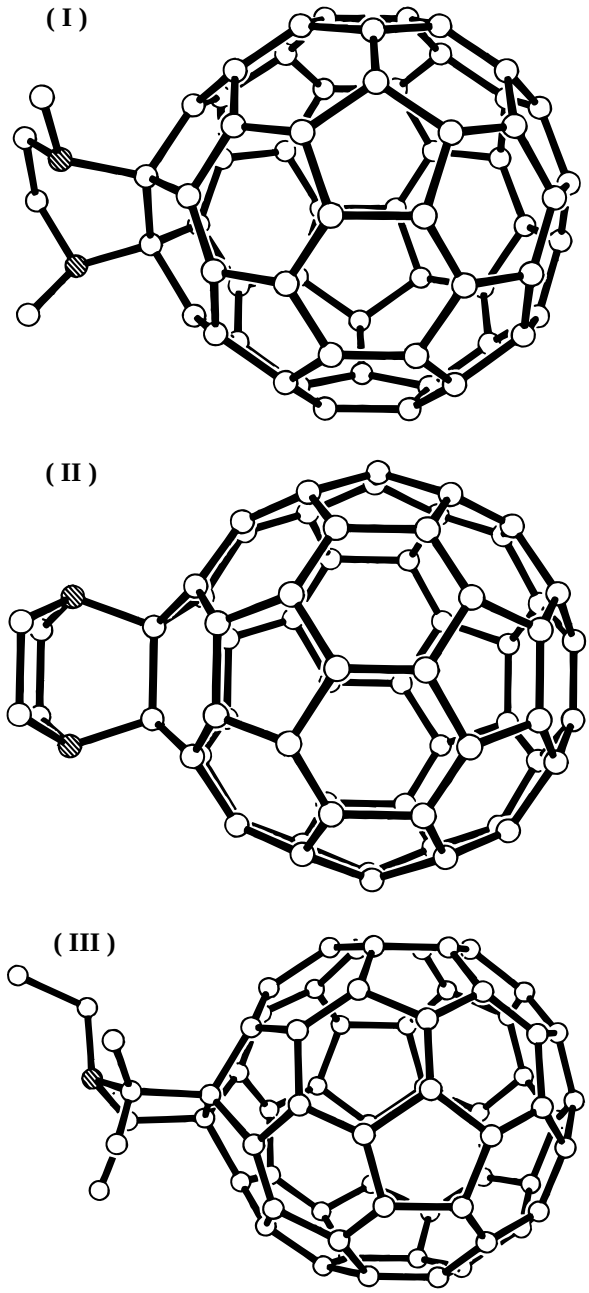

Figure 11. Optimized molecular structures of the amino-C_{60} derivatives **I** and **II** and the pyrrolidino-C_{60} derivative **III** obtained from ab initio (STO-3G) calculations.

absorption spectra of **I** and **II** are rather similar to that of the pyrrolidino-C_{60} derivative **III** in both spectral profile and absorptivity, except for the absence of a sharp peak in the 400−450 nm wavelength region (Figure 1). Other than minor solvatochromic shifts, absorption spectra of **I** and **II** are little changed from solvent to solvent. The solvent insensitivity of the absorption spectra reflects the fact that there are no meaningful changes in ground-state properties of the molecules in different solvents. The results also suggest no absorption contributions from any ground-state charge-transfer species.

Fluorescence spectra of the compound **I** in different solvents show only small changes, in sharp contrast to the wide variations in fluorescence quantum yield. The results suggest that observed fluorescence intensities in different solvents are likely due only to emissions from the vertical excited singlet state of the molecule. The strong dependence of fluorescence intensities on solvent polarity is likely correlated with different degrees

of excited-state quenching through electron transfer in solvents of different polarities. Since the solutions used in fluorescence measurements are very dilute ($<10^{-4}$ M), intermolecular interactions between amino-C_{60} molecules are negligible. The possibility of contributions from ground-state aggregates can also be ruled out. The amino-C_{60} derivatives are quite soluble in polar solvents such as chloroform and dichloromethane, much more so than the parent C_{60}. The fluorescence parameters of the derivatives in dichloromethane are independent of the sample concentrations (5×10^{-5} to 5×10^{-4} M). Thus, the fluorescence quenching for the compound **I** in polar solvents must be due to intramolecular n (amine unit) to π^* (C_{60} moiety) electron transfer. The involvement of n-orbital electrons in the electron-transfer process is made evident by the acidification effect (Table 1). For example, the fluorescence quantum yield of **I** in the toluene/acetonitrile (40%, v/v) mixture is less than 15% of that in neat toluene, but a small amount of TFA added to the solvent mixture essentially eliminates the fluorescence quenching. Since TFA only has a minor volume fraction in the solvent mixture, its effect as a solvent component other than acidity on molecular absorption and emission properties is insignificant. Fluorescence spectra and quantum yields of the pyrrolidino-C_{60} derivative **III** and methano-C_{60} derivatives are hardly different in solutions with and without TFA. The effect of acidifying the solution of **I** on observed fluorescence intensities is most likely associated with the protonation of amino groups in the molecule, which effectively shuts off the n$-\pi^*$ electron-transfer process. The acidification has only a minor effect on the absorption and fluorescence spectra of **I** because the electronic transitions in the C_{60} derivative are dictated by the monofunctionalized fullerene cage.

The optical limiting results of **I** in different solvents are consistent with the mechanism of excited singlet-state quenching through intramolecular n$-\pi^*$ electron transfer in a more polar solvent environment. For C_{60} in solution, optical limiting responses are due largely to the reverse saturable absorption mechanism.[36,37] The same mechanism is applicable to the optical limiting properties of C_{60} derivatives with the fullerene cage monofunctionalized.[29,30,38,39] Reverse saturable absorption occurs when the excited-state absorption cross sections (σ_S and σ_T) are larger than the ground-state absorption cross section (σ_G), $\sigma_{EFF}/\sigma_G > 1$, where σ_{EFF} includes a weighted average of σ_S and σ_T.[40] Because of their nanosecond intersystem crossing rate constants, optical limiting responses of C_{60} and the C_{60} derivatives toward 5$-$10 ns laser pulses are due predominantly to strong excited triplet-state absorptions. Thus, the factor σ_{EFF}/σ_G for evaluating the nonlinear absorption is reduced to $\Phi_{ISC}\sigma_T/\sigma_G$, where Φ_{ISC} denotes intersystem crossing quantum yields. For compound **I**, the weaker optical limiting responses in the chloroform/acetonitrile (20%, v/v) mixture (Figure 10) may be attributed to a decrease in the intersystem crossing yield due to intramolecular n$-\pi^*$ electron transfer as a competitive decay pathway of the excited singlet state. The acidification by adding TFA to the solvent mixture hinders the electron-transfer process, resulting in a significant improvement in the optical limiting performance.

For compound **I** in more polar solvents such as THF and dichloromethane, fluorescence decays are fast and the presence of a longer-lived component becomes evident. Because observed lifetimes of the longer-lived component (1.2$-$1.5 ns) are not so different from the lifetime of C_{60}, contribution due to residual C_{60} contamination was suspected. However, such a possibility was ruled out by comparing fluorescence decay results of the amino-C_{60} samples that had undergone different numbers of repeated purifications. Thus, the longer-lived fluorescence for **I** in polar solvents is likely associated with the electron-transfer process. Additional evidence is that the longer-lived component can be eliminated through acidifying the sample solution by adding a small amount of acid. The fluorescence decays of **I** in polar solvents in the presence of TFA are monoexponential, similar to those in nonpolar solvents (Figures 8). Since observed fluorescence spectra of **I** are hardly solvent dependent, the longer-lived component in fluorescence decays may not be assigned to charge-transfer excited-state emission as in TICT molecules.[4,5] Instead, it may tentatively be attributed to delayed emission from the vertical excited singlet state that is regenerated through back electron transfer. The excited-state processes of amino-C_{60} derivatives in polar solvents may be explained using the schematic energy diagram shown in Figure 12. For the compound **I**, the charge-transfer excited state is nonemissive, probably because the radiative process is slow compared to the excited-state lifetime. Fluorescence quantum yield and lifetime results of **I** obtained at different temperatures are consistent with such an explanation. For compound **I** in toluene without the photoinduced electron-transfer process, fluorescence quantum yields are temperature independent. However, in a more polar solvent environment in the toluene/acetonitrile (5%, v/v) mixture, fluorescence yields of **I** increase slightly with increasing temperature, whereas observed fluorescence lifetimes are essentially temperature independent (Figure 7). The higher fluorescence yields may be attributed to increasing contributions of the delayed emission because the regeneration of the vertical excited singlet state is more efficient at higher temperatures (Figure 12).

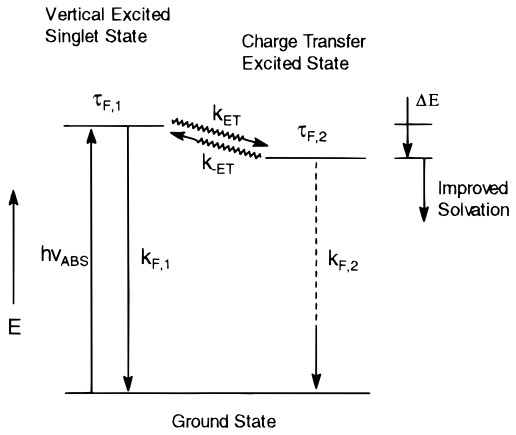

Figure 12. Schematic energy diagram for the intramolecular n$-\pi^*$ electron transfer in aminofullerene molecules.

The fluorescence properties of **II** are apparently even more solvent sensitive. Fluorescence quenchings are already significant for **II** in polarizable solvents such as toluene and CS_2 and even more so in polar solvents and solvent mixtures (Table 2). The extremely strong dependence of fluorescence quantum yields and decays of **II** on solvent polarity and polarizability may similarly be attributed to intramolecular n$-\pi^*$ electron transfer between the amino groups and the photoexcited fullerene cage. Similar to those of **I**, the excited-state processes of **II** may also be explained in terms of the schematic energy diagram in Figure 12, though the electron transfer is already a major excited-state decay process of **II** even in nonpolar but more polarizable solvents. A more significant difference between photoexcited-state properties of the two amino-C_{60} derivatives is that compound **II** has a second emissive excited state. The second emission observed for **II** in a polar or polarizable solvent environment is red-shifted from the fluo-

rescence band of the vertical excited singlet state. Because it can essentially be eliminated when the solution is acidified in the presence of TFA, the second emission may be assigned to the intramolecular n$-\pi^*$ charge-transfer excited state (Figure 12), namely that unlike in **I**, the radiative process in **II** is a competitive decay pathway of the n$-\pi^*$ charge-transfer excited state. The longer-lived component in observed fluorescence decays of **II** in polar and polarizable solvents may be contributed by emissions from both the charge-transfer excited state and the regenerated (delayed) vertical excited singlet state due to back electron transfer (Figure 12).

It is probably more than coincident that longer-lived emissions in **I** and **II** have similar lifetimes. The emissions originate from the charge-transfer excited states that are characteristic of the amino-C_{60} derivatives.

A comparison between the amino- (**I**, **II**) and pyrrolidino-C_{60} (**III**) derivatives is interesting. While compound **III** also has an amino group in the molecular structure, it undergoes no photoinduced intramolecular electron transfer even in a highly polar solvent environment. The obvious difference in photo-excited-state properties of the two kinds of C_{60} derivatives might be rationalized in terms of their different amino group(s)$-$fullerene cage relationships. With an assumption that the electron transfer originates in an excited-state geometry close to the Franck$-$Condon state, structural differences in the excited singlet states of the three compounds may be discussed using their optimized ground-state geometries. According to results from both semiempirical (MNDO) and ab initio (STO-3G minimum base set) calculations, the significant differences concerning amino group(s)$-$fullerene cage relationships are that the nitrogen$-$cage distance in **III** is slightly longer than those in **I** and **II** and that the electron lone pair on the nitrogen in **III** points away from the fullerene cage surface. Thus, intramolecular n$-\pi^*$ electron transfer through space is likely less favorable in **III** than in **I** and **II**. However, a more important structural difference between the two kinds of derivatives is that the amino nitrogen links to the fullerene cage through a bridge of two sp^3 carbons in **III** versus only one sp^3 carbon in **I** and **II**. The through-bond electron transfer should be more efficient in **I** and **II**.

The photoinduced intramolecular electron transfer in the amino-C_{60} derivatives **I** and **II** shares some characteristics with the excited-state processes in TICT molecules such that the electron transfer requires a polar solvent environment and that a charge-transfer excited state is formed as a result of the electron transfer.[4,5] However, a major difference is that the process in the amino-C_{60} derivatives involves no twisting between donor and acceptor moieties. In fact, the molecules **I** and **II** are better described as redox dyads in which the electron donor and acceptor units are linked directly through only an sp^3 carbon as a very simple spacer. It should be recognized that although amino groups (donor) are attached directly to the fullerene cage (acceptor) in the amino-C_{60} derivatives, there are no significant ground-state electronic interactions between the donor and acceptor units. The donor$-$acceptor relationship in **I** and **II** is different from those between the amino group and aromatic moiety in aniline derivatives and the TICT molecules represented by *N*,*N*-dimethylaminobenzonitrile.[3$-$5] In this regard, the intramolecular n$-\pi^*$ electron transfer discussed here is conceptually different from the TICT process, but similar to those in donor$-$spacer$-$acceptor supramolecules. Since the amino-C_{60} derivatives are effectively redox dyads with one of the simplest spacers, they may be used as models for more complex redox systems, particularly with respect to effects of the solvent environment on intramolecular electron-transfer processes.

The solvent dependence of photoinduced intramolecular n$-\pi^*$ electron transfer in the amino-C_{60} derivatives **I** and **II** may be discussed in a more quantitative fashion. The electron-transfer rate constants in different solvents and solvent mixtures may be estimated by assuming that other excited singlet-state processes are essentially solvent independent (with changes within error margins of fluorescence measurements).

$$k_{ET} = 1/\tau_{F,1} - 1/\tau_{F,hexane} \quad (1)$$

where $\tau_{F,1}$ represents observed fluorescence lifetimes of the vertical excited singlet state. Electron-transfer rate constants may also be estimated from observed fluorescence quantum yields if delayed emission contributions are relatively small (Figure 12). The results thus obtained show rather poor correlations with dielectric constants of the solvents (in plots of $1/\tau_{F,1}$ and $1/\Phi_F$ vs ϵ). The poor correlations are due at least in part to microscopic solvation effects, namely that the polarities microscopically experienced by the excited-state molecules in different solvents are different from the bulk polarities of the solvents as measured by dielectric constants. The microscopic polarities of solvents may be estimated using a solvatochromic molecular probe. To probe the microscopic solvent environment experienced by the amino-C_{60} molecules, an aminonaphthalene molecule 6-propionyl-2-(*N*,*N*-dimethylamino)naphthalene (PRODAN) was used. PRODAN has a molecular structure that is similar to those of classical TICT molecules, but it undergoes no TICT process in the excited state.[41] It is a highly fluorescent molecule, and the fluorescence spectrum is strongly solvatochromic. As a result, PRODAN has been widely employed in studies of microscopic domains in organic solvents and solvent mixtures, supercritical fluids, polymer membranes, and biological systems.[42$-$45]

For correlations of electron-transfer rate constants of the amino-C_{60} derivatives **I** and **II** with microscopic polarities in different solvents, fluorescence spectra of PRODAN were measured in the same series of solvents to determine solvatochromic shifts.

$$\tilde{\nu}_F = \tilde{\nu}_{F,0} + \Delta\tilde{\nu}_{F,S} \quad (2)$$

where $\Delta\tilde{\nu}_{F,S}$ represents fluorescence spectral shifts in different solvents. According to the classical solvation theory, $\Delta\tilde{\nu}_{F,S}$ has a linear relationship with the Onsager reaction field Δf, which is a function of the solvent dielectric properties.[46,47] In the same context, microscopic solvation effects on the solvatochromic probe may be considered by assuming that $\Delta\tilde{\nu}_{F,S}$ is linear with the average microscopic reaction field Δf_{MICRO}.[44,48] Similarly, the electron-transfer rate constants of the amino-C_{60} derivatives in different solvents may be related to the solvent microscopic polarities in ln k_{ET} vs Δf_{MICRO} correlations. Thus, the microscopic solvation dependence of the intramolecular n$-\pi^*$ electron transfer in **I** and **II** may be evaluated by correlating $\ln(1/\tau_{F,1})$ with the solvatochromic shifts $\Delta\tilde{\nu}_{F,S}$ of PRODAN in different solvents and solvent mixtures. Shown in Figure 13 is a plot of $\ln(1/\tau_{F,1})$ of **I** vs $-(\tilde{\nu}_F - \tilde{\nu}_{F,hexane})$ of PRODAN, where the negative sign indicates spectral shifts being bathochromic. The electron transfer is clearly more efficient in a microscopically more polar solvent environment, which corresponds to a larger bathochromic shift of the PRODAN fluorescence spectrum. However, the results in chloroform, dichloromethane, and *o*-dichlorobenzene are special, following a different trend (Figure

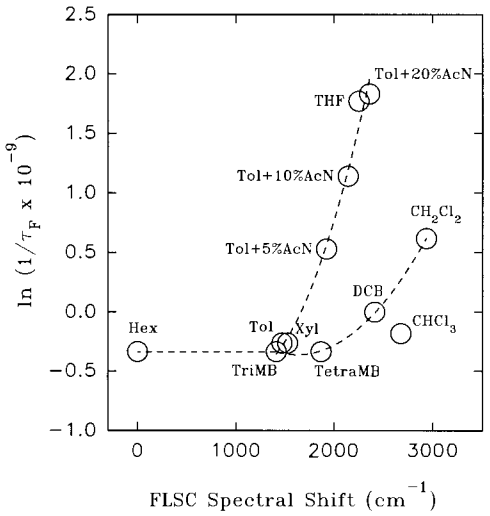

Figure 13. Correlation of $\ln(1/\tau_F)$ values of **I** with bathochromic fluorescence spectral shifts ($\tilde{\nu}_{F,hexane} - \tilde{\nu}_F$) of PRODAN under different solvent conditions.

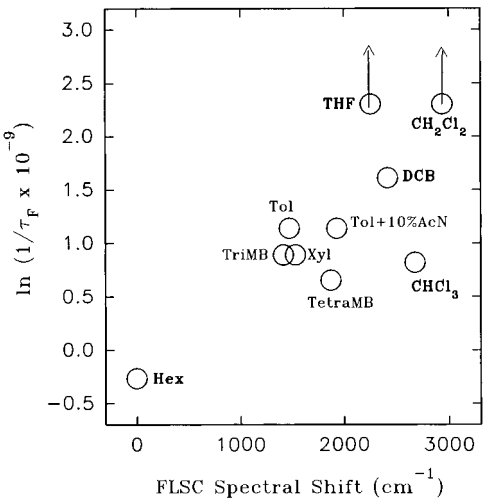

Figure 14. A correlation of $\ln(1/\tau_F)$ values of **II** with bathochromic fluorescence spectral shifts ($\tilde{\nu}_{F,hexane} - \tilde{\nu}_F$) of PRODAN under different solvent conditions.

13). It is probably no coincidence that these solvents are all chlorinated. There are two possible explanations for the results. One concerns the validity of the assumption that only the electron transfer is a solvent-dependent process in the excited singlet state. Since chlorine is a heavy atom, chlorinated solvents may change intersystem crossing quantum yields of the amino-C_{60} derivative. However, the heavy atom effect typically enhances intersystem crossing, making it more competitive with respect to other excited singlet-state processes. Consequently, the $1/\tau_{F,1}$ values in chlorinated solvents should be abnormally larger than those in solvents of comparable microscopic polarities but without heavy atoms, resulting in deviations that are opposite to those shown in Figure 13. Thus, the heavy atom effect is unlikely the principal cause for the results in chlorinated solvents. The second possible explanation is that there may be specific interactions between the excited-state amino-C_{60} and solvent molecules beyond microscopic solvation. Such specific interactions may hinder the intramolecular n$-\pi^*$ electron-transfer process, resulting in the kind of deviations shown in Figure 13.

A similar correlation can be made for the microscopic solvation dependence of electron transfer in **II**. Shown in Figure 14 is a plot of $\ln(1/\tau_{F,1})$ values of **II** vs fluorescence spectral shifts $-(\tilde{\nu}_F - \tilde{\nu}_{F,hexane})$ of PRODAN in different solvents. Qualitatively, the correlation in Figure 14 still indicates more efficient intramolecular electron transfer in **II** under microscopically more polar solvent conditions, which correspond to larger bathochromic shifts of the PRODAN fluorescence spectrum. Since the overall pattern for microscopic solvation effects on the intramolecular electron transfer in **II** is not so clear quantitatively, it is difficult to evaluate the results of **II** in chlorinated solvents in the same fashion as discussed above for **I**. Nevertheless, it seems that for **II,** in chloroform at least, the photoinduced intramolecular electron-transfer process is probably subject to special solvent effects beyond microscopic solvation.

The intramolecular n$-\pi^*$ electron transfer in the amino-C_{60} derivatives is clearly more efficient in a microscopically more polar solvent environment. The mechanism for solvation effects on the intramolecular electron transfer is an interesting issue. For both **I** and **II**, there are no electron-transfer processes in nonpolar solvents hexane and methylcyclohexane. A simple explanation is that the charge-transfer excited state is too high in energy compared to the vertical excited singlet state, namely there is not enough driving force for electron transfer. The same explanation has been used for TICT molecules in nonpolar solvents.[3−5] Interestingly, the same solvent dependence is also observed in fullerene−amine intermolecular systems. For example, the excited singlet states of C_{60} and C_{70} are essentially unquenched by triethylamine in hexane but strongly quenched in a polar solvent environment.[49] The intramolecular n$-\pi^*$ charge-transfer excited state is likely stabilized in polar solvents due to better solvation (Figure 12), which corresponds to stronger driving forces for the electron-transfer process. For both **I** and **II**, the intramolecular electron-transfer rate constants reach $\sim 1 \times 10^{10}$ s^{-1} (or even larger for **II**, Table 2) under highly polar solvent conditions. In addition to the driving force, solvent effects on the other factors in the expression of the electron-transfer rate constant[50,51] have to be considered for a more quantitative account. In this regard, the aminofullerene molecules may be employed in a quantitative modeling of solvation effects on intramolecular electron-transfer rate constants. More experimental measurements including fluorescence decays on a shorter time scale and transient absorptions of the charge-separated state are needed.

Acknowledgment. We thank Xian-Fu Zhang, Jason E. Riggs, and Harry W. Rollins for experimental assistance. Financial support from the National Science Foundation (CHE-9320558 and CHE-9727506) is gratefully acknowledged.

References and Notes

(1) (a) *Photoinduced Electron Transfer*; Fox, M. A., Chanon, M., Eds.; Elsevier: Amsterdam, 1988. (b) *Topics in Current Chemistry;* Mattay, J., Ed.; Springer-Verlag: Berlin, 1990−1994; Vols. 156, 158, 159, 163, 168, 169.

(2) (a) Wasielewski, M. R. *Chem. Rev.* **1992**, *92*, 435. (b) Speiser, S. *Chem. Rev.* **1996**, *96*, 1953.

(3) Rotkiewicz, K.; Grellman, K. H.; Grabowski, Z. R. *Chem. Phys. Lett.* **1973**, *19*, 315.

(4) (a) Rettig, W. *Angew. Chem., Int. Ed. Engl.* **1986**, *25*, 971. (b) Rettig, W. In *Topics in Current Chemistry* Mattay, J., Ed.; Springer-Verlag: Berlin, 1994; Vol. 169, p 253.

(5) (a) Lippert, E.; Rettig, W.; Bonačić-Koutecký, V.; Heisel, F.; Miehé, J. A. *Adv. Chem. Phys.* **1987**, *68*, 1. (b) Bhattacharyya, K.; Chowdhury, M. *Chem. Rev.* **1993**, *93*, 507.

(6) (a) Foote, C. S. In *Topics in Current Chemistry: Electron-Transfer I*; Mattay, J., Ed.; Springer-Verlag: Berlin, 1994; p 347. (b) Foote, C. S. In *Light Activated Pest Control*; ACS Symposium Series 616; American Chemical Society: Washington, DC, 1995; p 17.

(7) Jensen, A. W.; Wilson, S. R.; Schuster, D. I. *Bioorg. Med. Chem.* **1996**, *4*, 767.

(8) Sun, Y.-P. In *Molecular and Supramolecular Photochemistry*; Ramamurthy, V., Schanze, K. S., Eds.; Marcel Dekker: New York, 1997; Vol. 1, Chapter 9, p 325.

(9) Wang, Y. *J. Phys. Chem.* **1992**, *96*, 764.

(10) Williams, R. M.; Verhoeven, J. W. *Chem. Phys. Lett.* **1992**, *194*, 446.

(11) (a) Palit, D. K.; Ghosh, H. N.; Pal, H.; Sapre, A. V.; Mittal, J. P.; Seshadri, R.; Rao, C. N. R. *Chem. Phys. Lett.* **1992**, *198*, 113. (b) Seshadri, R.; Rao, C. N. R.; Pal, H.; Mukherjee, T.; Mittal, J. P. *Chem. Phys. Lett.* **1993**, *205*, 395. (c) Seshardi, R.; D'Souza, F.; Krishnan, V.; Rao, C. N. R. *Chem. Lett*. **1993**, 217. (d) Ghosh, H. N.; Pal, H.; Sapre, A. V.; Mittal, J. P. *J. Am. Chem. Soc.* **1993**, *115*, 11722.

(12) Sun, Y.-P.; Bunker, C. E.; Ma, B. *J. Am. Chem. Soc.* **1994**, *116*, 9692.

(13) Sun, Y.-P.; Ma, B. *Chem. Phys. Lett.* **1995**, *236*, 285.

(14) Park, J.; Kim, D.; Suh, Y. D.; Kim, S. K. *J. Phys. Chem*. **1994**, *98*, 12715.

(15) Ma, B.; Bunker, C. E.; Guduru, R.; Zhang, X.-F.; Sun, Y.-P. *J. Phys. Chem. A* **1997**, *101*, 5626.

(16) Sun, Y.-P.; Bunker, C. E.; Zhang, X.-F. Manuscript in preparation.

(17) (a) Williams, R. M.; Zwier, J. M.; Verhoeven, J. W. *J. Am. Chem. Soc.* **1995**, *117*, 4093. (b) Williams, R. M.; Koeberg, M.; Lawson, J. M.; An, Y.-Z.; Rubin, Y.; Paddon-Row, M. N.; Verhoeven, J. M. *J. Org. Chem.* **1996**, *61*, 5055.

(18) (a) Liddell, P. A.; Sumida, J. P.; Macpherson, A. N.; Noss, L.; Seely, G. R.; Clark, K. N.; Moore, A. L.; Moore, T. A.; Gust, D. *Photochem. Photobiol.* **1994**, *60*, 537. (b) Imahori, H.; Cardoso, S.; Tatman, D.; Lin, S.; Noss, L.; Seely, G. R.; Sereno, L.; De Silbert, J. C.; Moore, T. A.; Moore, A. L.; Gust, D. *Photochem. Photobiol*. **1995**, *62*, 1009. (c) Kuciauskas, D.; Lin, S.; Seely, G. R.; Moore, A. L.; Moore, T. A.; Gust, D.; Drovetskaya, T.; Reed, C. A.; Boyd, P. D. W. *J. Phys. Chem*. **1996**, *100*, 15926. (d) Liddell, P. A.; Kuciauskas, D.; Sumida, J. P.; Nash, B.; Nguyen, D.; Moore, A. L.; Moore, T. A.; Gust, D. *J. Am. Chem. Soc.* **1997**, *119*, 1400.

(19) (a) Imahori, H.; Hagiwara, K.; Akiyama, T.; Taniguchi, S.; Okada, T.; Sakata, Y. *Chem. Lett*. **1995**, 265. (b) Imahori, H.; Sakata, Y. *Chem. Lett*. **1996**, 199. (c) Imahori, H.; Hagiwara, K.; Aoki, M.; Akiyama, T.; Taniguchi, S.; Okada, T.; Shirakawa, M.; Sakata, Y. *J. Am. Chem. Soc*. **1996**, *118*, 11771.

(20) Sariciftci, N. S.; Wudl, F.; Heeger, A. J.; Maggini, M.; Scorrano, G.; Prato, M.; Bourassa, J.; Ford, P. C. *Chem. Phys. Lett*. **1995**, *247*, 510.

(21) Guldi, D. M.; Maggini, M.; Scorrano, G.; Prato, M. *J. Am. Chem. Soc.* **1997**, *119*, 974.

(22) (a) Drovetskaya, T.; Reed, C. A.; Boyd, P. *Tetrahedron Lett.* **1995**, *36*, 7971. (b) Ranasinghe, M. G.; Oliver, A. M.; Rothenfluh, D. F.; Salek, A.; Paddon-Row, M. N. *Tetrahedron Lett.* **1996**, *27*, 4797. (c) Nakamura, Y.; Minowa, T.; Hayashida, Y.; Tobita, S.; Shizuka, H.; Nishimura, J. *J. Chem. Soc., Faraday Trans.* **1996**, 377.

(23) Baran, P. S.; Monaco, R. R.; Khan, A. U.; Schuster, D. I.; Wilson, S. R. *J. Am. Chem. Soc.* **1997**, *119*, 8364.

(24) Sun, Y.-P.; Bunker, C. E.; Liu, B. *Chem. Phys. Lett.* **1997**, *272*, 25.

(25) Bunker, C. E.; Ma, B.; Rollins, H. W.; Sun, Y.-P. In *Fullerenes, Recent Advances in the Chemistry and Physics of Fullerenes and Related Materials;* Kadish, K. M., Ruoff, R. S., Eds.; The Electrochemical Society: Pennington, NJ, 1996; Vol. 4, p 308.

(26) Kampe, K.-D.; Egger, N.; Vogel, M. *Angew. Chem., Int. Ed. Engl*. **1993**, *32*, 1174.

(27) (a) Balch, A. L.; Cullison, B.; Fawcett, W. R.; Ginwalla, A. S.; Olmstead, M. M.; Winkler, K. *J. Chem. Soc., Chem. Commun*. **1995**, 2287. (b) Balch, A. L.; Ginwalla, A. S.; Olmstead, M. M. *Tetrahedron* **1996**, *52*, 5021.

(28) Lawson, G. E.; Kitaygorodskiy, A.; Ma, B.; Bunker, C. E.; Sun, Y.-P. *J. Chem. Soc., Chem. Commun.* **1995**, 2225.

(29) Sun, Y.-P.; Riggs, J. E. *Chem. Mater.* **1997**, *9*, 1268.

(30) Sun, Y.-P.; Lawson, G. E.; Riggs, J. E.; Ma, B.; Wang, N.; Moton, D. K. *J. Phys. Chem. A* **1998**, *102*, 5520.

(31) Ma, B.; Sun, Y.-P. *J. Chem. Soc., Perkin Trans. 2* **1996**, 2157.

(32) Anderson, J. L.; An, Y.-Z.; Rubin, Y.; Foote; C. S. *J. Am. Chem. Soc.* **1994**, *116*, 9763.

(33) Guldi, D. M.; Asmus, K.-D. *J. Phys. Chem. A* **1997**, *101*, 1472.

(34) Dewar, M. J. S.; Zoebisch, E. G.; Healy, E. F.; Stewart, J. J. P. *J. Am. Chem. Soc.* **1985**, *107*, 3902.

(35) Hehre, W. J.; Radom, L.; Schleyer, P. V. R.; Pople, J. A. *Ab Initio Molecular Orbital Theory*; Wiley: New York, 1985.

(36) Tutt, L. W.; Kost, A. *Nature* **1992**, *356*, 225.

(37) McLean, D. G.; Sutherland, R. L.; Brant, M. C.; Brandelik, D. M. *Opt. Lett.* **1993**, *18*, 858.

(38) Smilowitz, L.; McBranch, D.; Klimov, V.; Robinson, J. M.; Koskelo, A.; Grigorova, M.; Mattes, B. R.; Wang, H.; Wudl, F. *Opt. Lett.* **1996**, *21*, 922.

(39) (a) Maggini, M.; Scorrano, G.; Prato, M.; Brusatin, G.; Innocenzi, P.; Guglielmi, M.; Renier, A.; Signorini, R.; Meneghetti, M.; Bozio, R. *Adv. Mater*. **1995**, *7*, 404. (b) Signorini, R.; Zerbetto, M.; Meneghetti, M.; Bozio, R.; Maggini, M.; De Faveri, C.; Prato, M.; Scorrano, G. *J. Chem. Soc., Chem. Commun.* **1996**, 1891.

(40) Perry, J. W.; Mansour, K.; Lee, I.-Y. S.; Wu, X.-L.; Bedworth, P. V.; Chen, C.-T.; Ng, D.; Marder, S. R.; Miles, P.; Wada, T.; Tian, M.; Sasabe, H. *Science* **1996**, *273*, 1533.

(41) Bunker, C. E.; Bowen, T. L.; Sun, Y.-P. *Photochem. Photobiol.* **1993**, *58*, 499.

(42) (a) Weber, G.; Farris, F. J. *Biochemistry* **1979**, *18*, 3075. (b) Chong, P. L. *Biochemistry* **1988**, *27*, 399. (c) Chong, P. L.; Capes, S.; Wong, P. T. *Biochemistry* **1989**, *28*, 8358. (d) Zeng, J.; Chong, P. L. *Biochemistry* **1991**, *30*, 9485. (e) Sommer, A.; Paltauf, F.; Hermetter, A. *Biochemistry* **1990**, *29*, 11134. (f) Torgerson, P. M.; Drickamer, H. G.; Weber, G. *Biochemistry* **1979**, *18*, 3079. (g) Massey, J. B.; She, H. S.; Pownall, H. J. *Biochemistry* **1985**, *24*, 6973.

(43) (a) Betts, T. A.; Zagrobelny, J.; Bright, F. V. *J. Am. Chem. Soc.* **1992**, *114*, 8163. (b) Betts, T. A.; Zagrobelny, J.; Bright, F. V. *J. Supercrit. Fluids* **1992**, *5*, 48.

(44) Sun, Y.-P.; Bunker, C. E. *Ber. Bunsen-Ges. Phys. Chem.* **1995**, *99*, 967.

(45) Ma, B.; Bunker, C. E.; Simons, K.; Liu, J.-T.; Ma, J.-J.; Martin, C. W.; DesMarteau, D. D.; Sun, Y.-P. *J. Electroanal. Chem.* in press.

(46) Onsager, L. *J. Am. Chem. Soc.* **1936**, *58*, 1486.

(47) (a) Lippert, E. *Ber. Bunsen-Ges. Phys. Chem.* **1957**, *61*, 962. (b) Mataga, N.; Kubota, T. *Molecular Interactions and Electronic Spectra*; Marcel Dekker: New York, 1970.

(48) (a) Sun, Y.-P.; Fox, M. A.; Johnston, K. P. *J. Am. Chem. Soc.* **1992**, *114*, 1187. (b) Sun, Y.-P.; Bennett, G.; Johnston, K. P.; Fox, M. A. *J. Phys. Chem.* **1992**, *96*, 10002.

(49) Sun, Y.-P.; Ma, B.; Lawson, G. E. *Chem. Phys. Lett.* **1995**, *233*, 57.

(50) (a) Marcus, R. A. *J. Chem. Phys.* **1956**, *24*, 966. (b) Marcus, R. A. *Annu. Rev. Phys. Chem.* **1964**, *15*, 155.

(51) (a) Miller, J. R.; Calcaterra, L. T.; Closs, G. L. *J. Am. Chem. Soc.* **1984**, *106*, 3047. (b) Wasielewski, M. R.; Niemczyk, M. P.; Svec, W. A.; Pewitt, E. B. *J. Am. Chem. Soc.* **1985**, *107*, 1080.